



# Impact of soil-vegetation-atmosphere interactions on the spatial rainfall distribution in the Central Sahel

MARCUS BREIL\*, HANS-JÜRGEN PANITZ and GERD SCHÄDLER

Institute of Meteorology and Climate Research, Karlsruhe Institute of Technology (KIT), Germany

(Manuscript received August 12, 2016; in revised form December 22, 2016; accepted January 3, 2017)

## Abstract

In a Regional Climate Model (RCM) the interactions between the land surface and the atmosphere are described by a Soil-Vegetation-Atmosphere-Transfer Model (SVAT). In the presented study two SVATs of different complexity (TERRA-ML and VEG3D) are coupled to the RCM COSMO-CLM (CCLM) to investigate the impact of different representations of soil-vegetation-atmosphere interactions on the West African Monsoon (WAM) system. In contrast to TERRA-ML, VEG3D comprises a more detailed description of the land-atmosphere coupling by including a vegetation layer in its structural design, changing the treatment of radiation and turbulent fluxes. With these two different model systems (CCLM-TERRA-ML and CCLM-VEG3D) climate simulations are performed for West Africa and analyzed. The study reveals that the simulated spatial distribution of rainfall in the Sahel region is substantially affected by the chosen SVAT. Compared to CCLM-TERRA-ML, the application of CCLM-VEG3D results in higher near surface temperatures in the Sahel region during the rainy season. This implies a southward expansion of the Saharian heat-low. Consequently, the mean position of the African Easterly Jet (AEJ) is also shifted to the south, leading to a southward displacement of tracks for Mesoscale Convective Systems (MCS), developing in connection with the AEJ. As a result, less precipitation is produced in the Sahel region, increasing the agreement with observations. These analyses indicate that soil-vegetation-atmosphere interactions impact the West African Monsoon system and highlight the benefit of using a more complex SVAT to simulate its dynamics.

**Keywords:** West African Monsoon, Soil-vegetation-atmosphere interaction, Land surface-atmosphere coupling, Regional Climate Modeling

## 1 Introduction

The effects of anthropogenic climate change will continue to alter the human living conditions all over the world. This is in particular true for regions like the West African Sahel, in which the economical, political and social development strongly depends on agriculture. In this area the livelihood and the food security is closely connected to the yearly arrival of the West African Monsoon (WAM) (BENSON and CLAY, 1998). Thus, a decrease in the annual rainfall amount, as observed during the Sahel drought in the last century (NICHOLSON, 2013), can have extensive social-economic effects (MORTIMORE, 1989). To reduce the negative impact of such events in future, reliable information about the near future climate conditions are essential to plan and take appropriate adaptation measures. Therefore, a better understanding of the WAM dynamics and its mechanisms is required.

In this context the soil and vegetation characteristics influence the climate conditions by affecting the radiation budget of the surface and controlling the exchange of latent and sensible heat between the ground and the atmosphere. Results from KOSTER et al. (2004)

showed that these characteristics play a crucial role for the climatic conditions in the West African Sahel. In particular they affect the formation of convective rainfall events in the Sahel region (ADLER et al., 2011; GANTNER and KALTHOFF, 2010), where the spatial distribution of soil moisture and plant cover is very heterogeneous. In regions with wet soils the latent heat fluxes are increased in comparison to dry soil areas (PHILIPPON and FONTAINE, 2002). In consequence, the Convective Available Potential Energy (CAPE) rises within the planetary boundary layer (SCHÄR et al., 1999), and the frequency and the intensity of convective rainfall events are enhanced (PAL and ELTAHIR, 2001). Furthermore, the albedo of such wet soils is decreased, resulting in a higher absorption of short-wave radiation (PHILIPPON and FONTAINE, 2002) and thus in a stronger heating of the soil. This, in turn, raises the sensible heat fluxes and again a higher CAPE is reached. Additionally, different plant types and coverage can have similar effects on the conditions within the boundary layer, by revealing deviating transpiration rates, due to variant root depths (TEULING et al., 2006), for instance.

In the Sahel, convective rainfall, developing in Mesoscale Convective Systems (MCS), contributes substantially to the yearly amount of precipitation (LEBEL et al., 2003). The development of MCS is strongly coupled to the African Easterly Jet (AEJ) (REED et al., 1977).

\*Corresponding author: Marcus Breil, Institute of Meteorology and Climate Research, Karlsruhe Institute of Technology (KIT), Germany, e-mail: marcus.breil@kit.edu

The AEJ is built by the large temperature gradient between the warm air above the African continent in the north and the cooler air masses above the tropical Atlantic ocean in the south between April and November (NICHOLSON and GRIST, 2003). The Jet develops at the boundary of these two air masses at about 15° N in 600–700 hPa, with its strongest phase in June. During this time the average wind speed in the core region is about 12 m/s (NICHOLSON and GRIST, 2003). Because of instabilities within the Jet, ‘African Easterly Waves’ (AEW) develop. In the troughs of these waves the monsoon flow transports humid air from south-west into the Sahel, increasing the CAPE in the lower atmosphere (TAYLOR et al., 2005). Because of the overlying AEJ and its strong easterly winds, high vertical wind shear can be observed (HOLTON and HAKIM, 2013), favouring the formation of MCS. These MCS subsequently travel along with the mean AEJ stream from east to west over the Sahel region.

LARE and NICHOLSON (1994) showed that the interactions between soil, vegetation and atmosphere influence the characteristics of the AEJ. They analysed a transect of measuring stations and showed that the amount of latent heat fluxes affects the temperature gradient between the warm continent and the cooler ocean and thus the intensity of the AEJ. STEINER et al. (2009) used a more sophisticated Soil-Vegetation-Atmosphere-Transfer Model (SVAT) within Regional Climate Model (RCM) simulations and demonstrated that a more complex representation of the soil-vegetation-atmosphere interactions improved the simulated rainfall over West Africa. In this context, a more realistic position of the AEJ was simulated.

This paper will further investigate the impacts of soil-vegetation-atmosphere interactions on the characteristics of the AEJ and thus the MCS formation. Additionally, the question is answered whether a more complex representation of these interactions within a RCM improves the simulation of the WAM and in consequence of the sahelian rainfall. For that purpose, regional climate simulations with the RCM COSMO-CLM (CCLM) (ROCKEL et al., 2008) are performed, using the two different Soil-Vegetation-Atmosphere-Transfer Models TERRA-ML (SCHRODIN and HEISE, 2002) and VEG3D (BRAUN and SCHÄDLER, 2005). The coupling of VEG3D to CCLM was done via the OASIS3-MCT coupling software (VALCKE et al., 2013). TERRA-ML is the standard SVAT of CCLM, implemented as a subroutine. The model setup and short descriptions of the models used, and the simulations performed, are given in Section 2. Afterwards, in Section 3, the influence of the soil-vegetation-atmosphere interactions on the spatial rainfall variability in the Sahel is demonstrated in detail for a representative example. In Section 4 the relevance of these interactions on the WAM is evaluated on a decadal timescale, and the added value of using VEG3D compared to the usage of TERRA-ML is presented. Finally, conclusions are drawn in Section 5.

## 2 Models, model setups and simulations performed

### 2.1 CCLM

CCLM is the climate version of the nonhydrostatic weather forecast model COSMO (Consortium for Small-scale Modeling, DOMS et al. (2011), BALDAUF et al. (2011)) of the German Weather Service (DWD). In this study, CCLM version COSMO-4.21-CLM2 is applied. The model solves the hydro-thermodynamical equations describing compressible motions in a moist atmosphere. These equations are discretized on a three-dimensional Arakawa-C grid (ARAKAWA and LAMB, 1977) based on rotated geographical coordinates and a generalized, terrain following height coordinate. The numerical time integration is done by a Runge-Kutta scheme (WICKER and SKAMAROCK, 2002). The prognostic variables are: horizontal and vertical wind components, temperature, pressure perturbation, specific humidity, cloud water and cloud ice content and the specific water content of rain and snow.

Within CCLM a set of physical parameterizations is included to describe sub-grid processes. This comprises the radiative transfer scheme by RITTER and GEYLEN (1992) and the Tiedtke parameterization of convection (TIEDTKE, 1989). Turbulence is parameterized according to RASCHENDORFER (2001), using a level 2.5 closure for Turbulent Kinetic Energy (TKE) as prognostic variable (MELLOR and YAMADA, 1982). Cloud microphysics are represented by a reduced version of the one-moment scheme of SEIFERT and BEHENG (2001). A detailed description of CCLM and its dynamics, physics and numerics can be found in DOMS et al. (2011). For the study described in this paper a model setup was used, which was developed and evaluated within the framework of the Coordinated Regional Climate Downscaling Experiment for Africa (CORDEX Africa, (PANITZ et al., 2014)).

### 2.2 SVAT

Within a RCM the interactions between soil, vegetation and atmosphere are simulated in a SVAT. The SVAT calculates the impact of the atmospheric input (wind, temperature, pressure, incoming short- and longwave radiation, and precipitation) on the soil and surface conditions. Equations describing the transport of heat and water from the surface to the deep soil and vice versa are solved numerically. Based on the resulting soil conditions, sensible and latent heat fluxes between the surface and the atmosphere are calculated. These fluxes are needed as lower boundary conditions in the RCM.

#### 2.2.1 TERRA-ML

TERRA-ML (SCHRODIN and HEISE, 2002) is the standard SVAT implemented in CCLM. To calculate the vertical distribution of temperature within the soil, TERRA-ML solves the heat conduction equation by using finite

differences. In this study, the soil column is discretized into ten non equidistant levels with the bottom of the deepest layer at 15.34 m. In this layer a prescribed climatological temperature is used as lower boundary condition. The soil heat flux, derived from the energy balance at the surface, defines the upper boundary condition. The soil water content in each layer is calculated by solving the Richards equation. In the deepest layer of the model gravitational drainage takes place, while precipitation, dew and rime constitute the water input through the soil surface. Rainfall on vegetation is collected in an interception reservoir, snowfall in an additional snow layer. Evapotranspiration is computed based on the BATS model according to [DICKINSON \(1984\)](#).

### 2.2.2 VEG3D

VEG3D is an additional SVAT that can be used in connection with CCLM, replacing TERRA-ML. It was developed by [SCHÄDLER \(1990\)](#) at the Karlsruhe Institute of Technology (KIT), based on a model designed by [DEARDORFF \(1978\)](#). Further developments were performed by [LENZ \(1996\)](#), [GRABE \(2002\)](#), [BRAUN \(2005\)](#) and [MEISSNER \(2008\)](#). The SVAT was evaluated in several studies, e.g. by [BRAUN and SCHÄDLER \(2005\)](#) and [KÖHLER et al. \(2012\)](#).

Similar to TERRA-ML, VEG3D solves the heat conduction equation and the Richards equation by using finite-difference-methods, applying the same soil layer structure down to a depth of 15.34 m. The boundary conditions for VEG3D are also calculated by the atmospheric part of CCLM. However, both SVATs differ in the representation of the soil-vegetation-atmosphere interaction. In the following section these differences are summarized.

### 2.2.3 Differences between TERRA-ML and VEG3D

#### Parameterization of soil processes

In order to solve the Richards equation the hydraulic conductivity of an unsaturated soil needs to be parameterized. For this purpose, an approach of [RIJTEMA \(1969\)](#) is used within TERRA-ML, whereas in VEG3D the parameterization of [VAN GENUCHTEN \(1980\)](#) is applied. The models differ also with respect to the dependency of the heat conductivity on soil water content. In VEG3D the heat conductivity is influenced by the presence of water, this is not the case for the TERRA-ML version used in this study. VEG3D uses an approach of [JOHANSEN \(1977\)](#) to derive the heat conductivity depending on soil water content and soiltype while within TERRA-ML a constant value is used for each soiltype. A more recent version of TERRA-ML takes into account also this dependency. Its impact on the simulation results is discussed in Section 5.

#### Radiation fluxes

The main difference in the structural design of both SVATs is constituted in the existence of an explicit vegetation layer, which is taken into account in VEG3D, but

not in TERRA-ML. This vegetation layer is designed as one homogeneous and massless big leaf, located between the lowest atmospheric level and the surface. Wherever vegetation appears, incoming short-wave radiation is reflected and absorbed by the vegetation layer, and long-wave radiation is emitted back to the atmosphere and down to the soil, depending on the temperature within the vegetation layer. Thus, the radiation fluxes are calculated for both vegetated and non-vegetated areas. In TERRA-ML the complete radiation budget is simulated without considering shading effects due to vegetation.

#### Turbulent fluxes

In case of vegetation, the exchange of sensible and latent heat between the surface and the atmosphere is regulated by the vegetation layer implemented in VEG3D. This layer has its own canopy temperature and specific humidity, calculated iteratively from the canopy energy balance. Based on these values the vertical turbulent mixing is parameterized according to the gradients between the surface, the canopy and the lowest atmospheric level, using the Monin-Obuchov similarity theory ([STULL, 2012](#)). This theory is also used in TERRA-ML in connection to the TKE-based turbulent mixing scheme ([RASCHENDORFER, 2001](#)) to calculate the turbulent fluxes. But in contrast to VEG3D, TERRA-ML does not distinguish between vegetated and non-vegetated areas. A summary of the characteristics of both SVATs is listed in Table 1.

### 2.3 OASIS3-MCT

The coupling between CCLM and VEG3D is organized via the OASIS3-MCT software, developed by the ‘Centre Européen de Recherche et de Formation Avancée en Calcul Scientifique’ (CERFACS) in Toulouse, France ([VALCKE et al., 2013](#)). OASIS is a software that is widely used in the climate modeling community to couple models representing different parts of the climate system with each other like atmosphere-, ocean- and soil-vegetation-models ([VALCKE, 2013](#)).

In the current OASIS3-MCT version, the OASIS coupler is combined with the Model Coupling Toolkit (MCT), developed by the Argonne National Laboratory, USA ([LARSON et al., 2005](#)). OASIS3-MCT works as a library that is linked to CCLM and VEG3D. The coupling interface of VEG3D is part of the unified OASIS interface in CCLM ([WILL et al., submitted](#)). The main task of the coupler is to exchange and, if necessary, interpolate the fields between CCLM and VEG3D to establish a coupled system ([VALCKE et al., 2013](#)). The communication between the coupled models is managed via the Message Passing Interface (MPI) library.

### 2.4 Simulations performed

For this study CCLM simulations using both SVATs (CCLM-TERRA-ML and CCLM-VEG3D) are performed for two different time periods. In a first experiment a sensitivity analysis is executed and evaluated for



**Table 1:** structural design of TERRA-ML and VEG3D.

	TERRA-ML	VEG3D
Number of soil layers	10	10
Depth of deepest layer	15.34 m	15.34 m
Thermal calculation	heat conduction equation	heat conduction equation
Thermal conductivity of the soil	independent on soil water content	depend on soil water content
Lower boundary condition for temperature	climatological temperature in deepest layer	climatological temperature in deepest layer
Hydrological calculation	Richards equation	Richards equation
Parameterization of soil water transport	RIJTEMA (1969)	VAN GENUCHTEN (1980)
Lower boundary condition for hydrology	gravitational drainage	gravitational drainage
Vegetation	no vegetation layer included	vegetation layer included
Radiation fluxes	shading not considered	shading considered
Turbulent fluxes	calculated by surface values	calculated by values inside the canopy

one selected year. To get a representative image of the processes within the West African monsoon system, the selected year needs to be one of average monsoon dynamics, and consequently exhibit average precipitation amounts. Figure 1 shows the anomalies in yearly precipitation in the Central Sahel region with respect to the 1950–2001 mean for the gridded datasets of the University of Delaware (UDEL) (WILLMOTT and MATSUURA, 1998) and the Climatic Research Unit (CRU) (University of East Anglia, MITCHELL and JONES (2005)). The region Central Sahel (CS) (Figure 2) is adapted to a climatological region defined by NICHOLSON and PALAO (1993). In 1979 the deviation to the longterm mean is minimal in both observational datasets and this year is considered representative for the last 50 years. Thus, it is selected as simulation year for the sensitivity analysis. Based on the results of the one year simulations, the impact of the soil-vegetation-atmosphere interactions on the West African Monsoon system is analysed and presented in Section 3. Afterwards, the relevance of major processes being identified is validated on a longer time scale in a second experiment. In this context, CCLM simulations applying both SVATs are performed for the decade 2001–2010.

The model domain used in the experiments expands from 60.28° West to 60.28° East and from 45.32° South to 45.32° North (Figure 2). The horizontal grid spacing is 0.44°, thus the model domain comprises 275 grid points from West to East and 207 gridpoints from South to North. In the vertical the atmosphere is discretized in 35 levels, with the uppermost layer at 30 km height above sea level. A time step of 240 seconds is used for the numerical solution of the prognostic equations in CCLM as well as for the coupling between CCLM and VEG3D. The simulations are driven by ERA-Interim Reanalysis (DEE et al., 2011) at the lateral boundaries and at the lower boundary over sea. To achieve balanced soil temperatures and water contents for the initialization of the different simulations, a transient CCLM run using TERRA-ML (1960–2010), had been performed. This transient run was driven by ERA40 (UPPALA et al., 2005) for the period 1960–1979, and ERA-Interim for the period 1979–2010. To ensure comparability, the CCLM simulations coupled to VEG3D, were also ini-

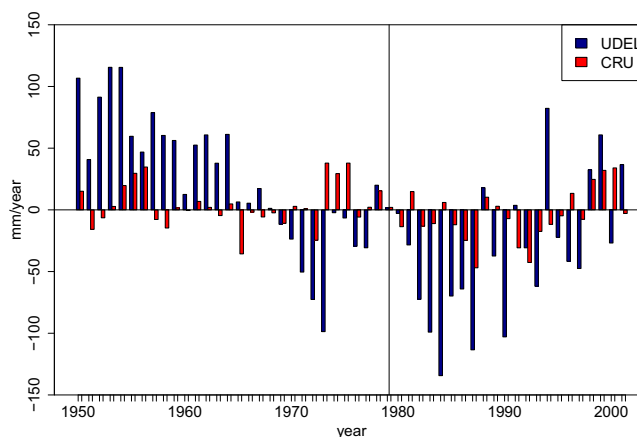


**Figure 1:** Anomalies of yearly precipitation sum in the Central Sahel with respect to 1950–2001 in [mm/year], derived from the gridded observational datasets of the University of Delaware (UDEL, blue) (WILLMOTT and MATSUURA, 1998) and the Climatic Research Unit (CRU, red) (MITCHELL and JONES, 2005). The year 1979 is marked with the vertical line. The Central Sahel region is adapted to a climatological region defined by NICHOLSON and PALAO (1993).

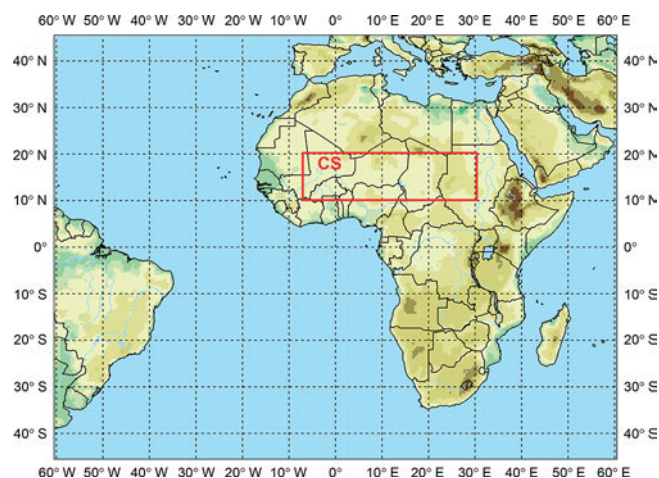


**Figure 2:** Model domain including the evaluation region Central Sahel (CS), highlighted in red. CS is adapted to a climatological region defined by NICHOLSON and PALAO (1993).

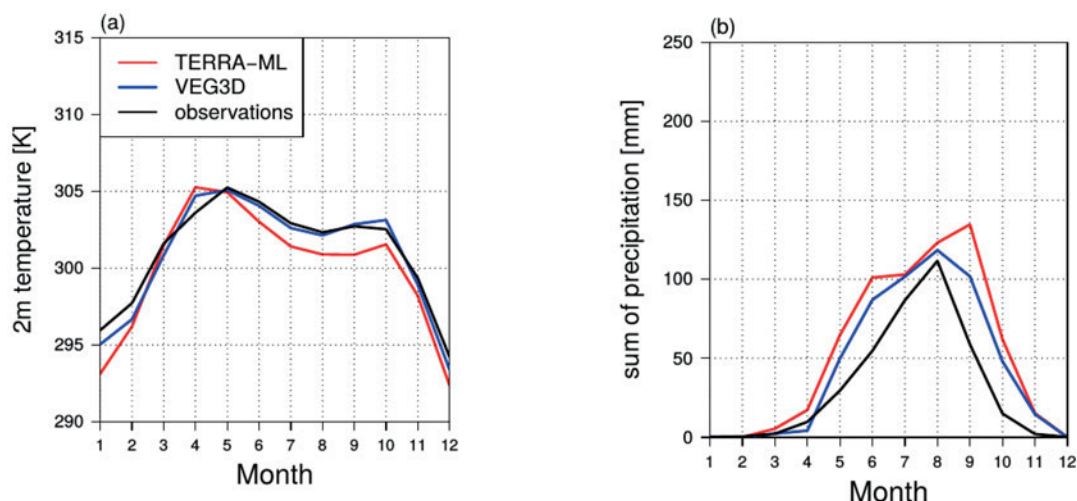


**Figure 3:** Annual cycle of area averaged monthly mean 2 m temperatures (a) and monthly mean precipitation sum (b) in Central Sahel in the year 1979. The red line shows the result of the CCLM-TERRA-ML simulation, the blue one the result of the CCLM-VEG3D simulation. UDEL is given in black.

tialized with these initial conditions. For both SVATs, land use classes were derived from the GLC2000 dataset (BARTHOLOME and BELWARD, 2005), and soiltypes from the ECOCLIMAP-2 dataset (KAPTUE TCHUENTE et al., 2010).

To evaluate the simulation results a set of observational data is available for West Africa. The available ground observations and satellite products last over different time periods and all exhibit a certain degree of uncertainty (PANITZ et al., 2014). In the framework of this study, taking into account the above mentioned transient CCLM run, a long time span is simulated. Therefore, the observations used for evaluation have to cover the same long time period. The gridded datasets of UDEL, CRU, and the Global Precipitation Climatology Centre (RUDOLF et al., 2010) meet this criterion (PANITZ et al., 2014). In general, all three datasets agree very well with each other (ZHANG et al., 2012), although each dataset has its own characteristics as shown in Figure 1 for the UDEL and the CRU data. In PARKER et al. (2012), UDEL in its  $0.5^\circ$  grid spacing and monthly temporal resolution is recommended. Because of that and for the sake of clarity, in the following only UDEL is used in this study.

### 3 Results of the sensitivity study

In a first step, the impact of the soil-vegetation-atmosphere interactions and their representation in two different SVATs on the WAM were investigated. Two ERA-Interim driven simulations with CCLM were performed for the year 1979. One, named CCLM-TERRA-ML, used CCLM's standard SVAT TERRA-ML, for the second one, named CCLM-VEG3D, VEG3D had been coupled to CCLM. Figure 3 shows the annual cycle of the simulated monthly and spatially averaged 2 m temperatures (a) and precipitation sums (b) for the Central Sahel in comparison to UDEL. The diagrams show that for

both variables, temperature and precipitation, the simulated annual cycle differ substantially. Especially in the middle of the year (June–October), the 2 m temperatures of the CCLM-VEG3D simulation (red curve) are remarkably higher than in the CCLM-TERRA-ML simulation (blue curve) and match the observations (black curve) much better. Also the general wet bias in the simulated monthly precipitation sums is considerably reduced in the CCLM-VEG3D run.

These differences in the simulation results must be caused by the use of the different SVATs, because all other boundary conditions were identical in both simulations. As described in Section 2.2.3, the representation of the soil-vegetation-atmosphere interaction is quite different between TERRA-ML and VEG3D. This means, that these interactions have a clear impact on the near surface temperature and the precipitation sum in the Sahel region, and using VEG3D reduces the temperature and precipitation bias substantially (Figure 3).

The higher near surface temperature in the CCLM-VEG3D simulation in the middle of the year leads to a reduction of the surface pressure in the Central Sahel region, causing the development of a stronger heat-low in this area, which also expands farther to the south than in the CCLM-TERRA-ML simulation. This effect is strongest in September (Figure 4) and it has further physical impacts, which are exemplarily described for September in the following paragraph.

Due to the more intense heat-low over the Central Sahel, the warm air mass over North Africa is extended southward in the CCLM-VEG3D simulation (Figure 4). To highlight this southward shift, in Figure 4(b) the 299 K isothermes of both simulations are drawn additionally. It can be seen that the 299 K isotherme in CCLM-VEG3D (solid white line) is located farther south than in CCLM-TERRA-ML (dotted black line). Thus, the boundary between the warm air mass over the Sahara and the cooler air mass over the tropical Atlantic

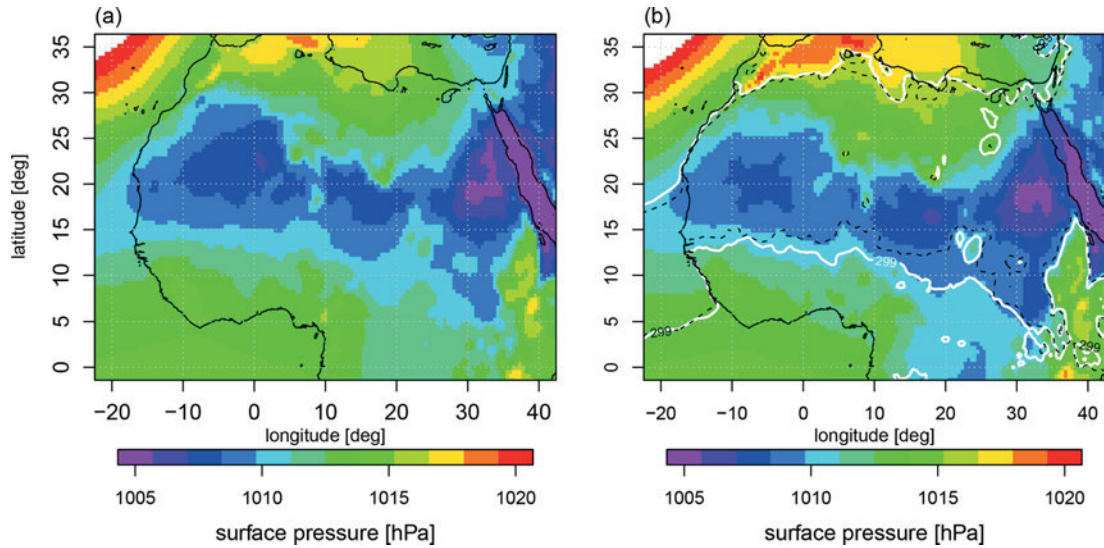


**Figure 4:** Surface pressure [hPa] in September 1979 for the CCLM-TERRA-ML (a) and the CCLM-VEG3D simulations (b). To highlight the southward shift of the heat-low in CCLM-VEG3D, the 299 K isothermes of both simulations are additionally drawn in (b) as a black dotted line for CCLM-TERRA-ML and a solid white line for CCLM-VEG3D.

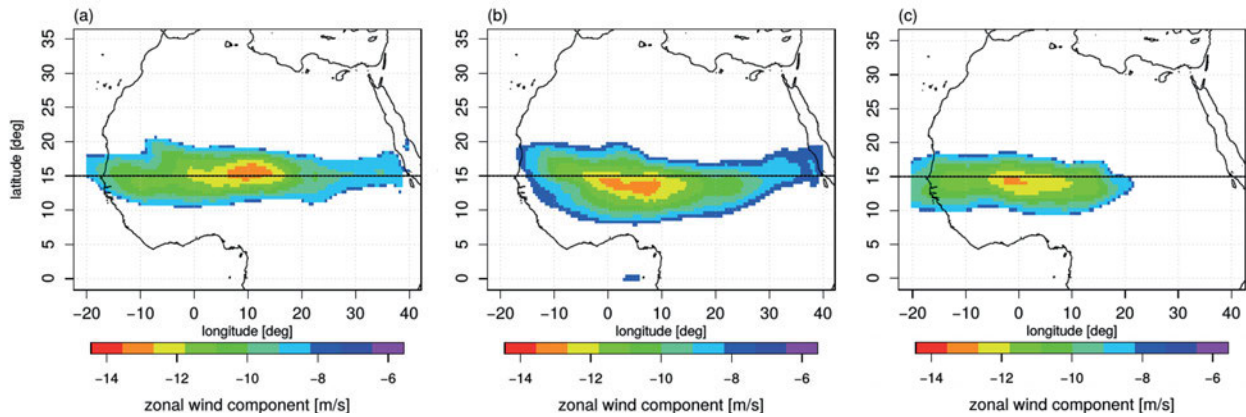


**Figure 5:** 95-percentile of the easterly wind components in 600 hPa for the CCLM-TERRA-ML (a), the CCLM-VEG3D simulations (b) and ERA-Interim (c). For reasons of clarity the westerly wind components are not shown and an auxiliary line in the middle of CS is drawn at 15° N to improve the comparability of the three AEJ positions.

ocean, at which the AEJ is formed, is also shifted to the south, with the consequence, that the jet is located farther south than in the CCLM-TERRA-ML simulation. This behaviour is demonstrated in Figure 5. It shows, for both simulations and the ERA-Interim Reanalysis, the 95-Percentile of the zonal wind component in 600 hPa, representing the mean position of the AEJ. In CCLM-TERRA-ML the core of the AEJ is situated north of 15° N (center latitude of CS), but in CCLM-VEG3D it is shifted to the south and the latitudinal AEJ position in the CCLM-VEG3D simulation is similar to its position derived from the ERA-Interim reanalysis, which is also located south of 15° N.

Because of this southward displacement of the AEJ in the CCLM-VEG3D simulation, the AEWs develop in a more southerly location as well, and move on more southerly tracks over the Sahel region. According to this MCSs, developing in the troughs of these waves, are also formed farther south. To track the position of these

MCSs, the locations of the daily rainfall maxima in West Africa are detected in both simulations and compared to each other. In Figure 6 the tracks of MCSs developed in September 1979, are illustrated. The MCS tracks for CCLM-VEG3D are drawn in blue and for CCLM-TERRA-ML in red. The southward shifted MCS positions are clearly visible in the CCLM-VEG3D results.

Since precipitation is closely related to the occurrence of MCSs, the southward shift of such systems in CCLM-VEG3D lead to less rainfall in the northern parts of the Central Sahel and to more in the southern parts (Figure 7). Figure 7 shows the difference in monthly precipitation sums between the CCLM-TERRA-ML and the CCLM-VEG3D simulations. Reddish colours represent positive differences, indicating that the CCLM-TERRA-ML simulation produces more rainfall in the northern areas. Blue colours, depicting negative differences, occur mostly in the southern areas in which the precipitation of the CCLM-VEG3D simulation is stronger. Due



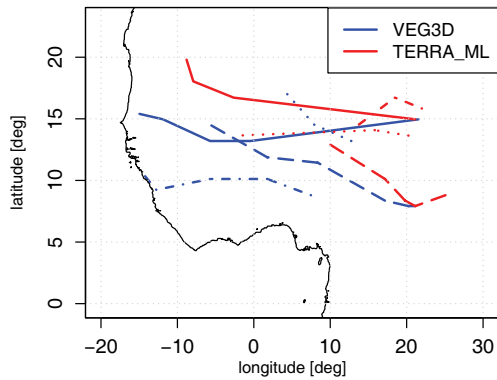


**Figure 6:** MCS tracks in September 1979 for the CCLM-TERRA-ML (red) and the CCLM-VEG3D (blue) simulations. The temporally corresponding tracks in the different simulations are drawn in the same line type. The convective systems are tracked by the latitudinal locations of the daily rainfall maxima in West Africa.

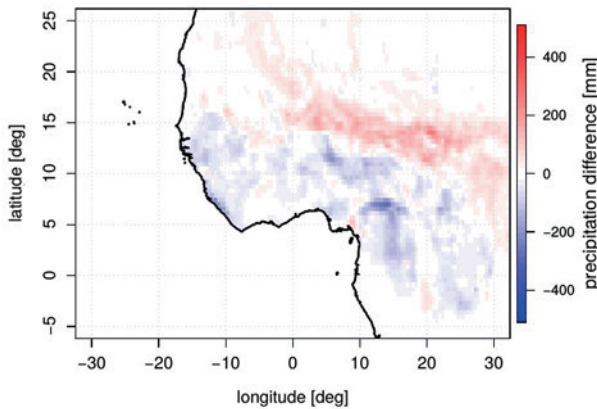


**Figure 7:** Differences in precipitation in September 1979 between the CCLM-TERRA-ML and the CCLM-VEG3D simulations in [mm].

to the southward displacement of simulated rainfall in the CCLM-VEG3D simulation compared to the CCLM-TERRA-ML run, less rainfall is produced in the Central Sahel region with the consequence that CCLM-VEG3D matches much better to the observations (Figure 3 (b)). The whole chain of physical processes described above reveals that the interactions between soil, vegetation and atmosphere considerably affect the spatial distribution of rainfall in the Sahel region, and that they must be modeled as realistic as possible.

## 4 Results for the decadal run

In a second step, ERA-Interim driven CCLM simulations were performed over decade 2001–2010 using the same model setup as for the sensitivity study described in Section 3. Figure 8 shows the spatially averaged annual cycle of the 2 m temperature (a) and the precipitation sums (b) for the Central Sahel, simulated with CCLM-VEG3D (red curve) and CCLM-TERRA-ML (blue curve). Again UDEL is used for the comparison with observations. The results show the same

characteristics as for the one year run for 1979. In the middle of the year higher 2 m temperatures are simulated in the CCLM-VEG3D run (about 1 K higher), and they agree well with observations (Figure 8 (a)). Furthermore, the observed general wet bias is reduced in the CCLM-VEG3D simulation (Figure 8 (b)), discussed later in this section. These characteristics can be observed in each single year of the decade 2001–2010 (not shown). Thus, also on the decadal timescale the soil-vegetation-atmosphere interactions have an impact on the near surface temperatures and the precipitation sums in the Central Sahel. And, consequently, the chain of processes takes place in a similar manner as described in Section 3.

The resulting southward displacement of the MCS tracks in CCLM-VEG3D over the decade 2001–2010 is shown in Figure 9. The tracks are represented by the latitudinal location of the daily rainfall maxima in all September months of the decade, summarized in boxplots. The thick black line indicates the mean position of the daily rainfall maxima in West Africa and the grey box comprises the 25- and the 75-Percentile. The whole spread of occurring positions is defined by the thin black lines. During the decade 2001–2010 the mean latitude of the daily rainfall maxima in CCLM-VEG3D is 11.7° N, in contrast to 12.5° N in the CCLM-TERRA-ML simulation. But not only the mean position in CCLM-VEG3D is shifted to the south, also the majority of the MCS tracks have a more southerly location, indicated by the grey box.

The averaged southward shift of the main area of rainfall compared to the CCLM-TERRA-ML run is highlighted in Figure 10. This deviating spatial rainfall distribution of the CCLM-VEG3D simulation reduces the bias of the monthly precipitation sum in September over the whole decade in contrast to the CCLM-TERRA-ML run, as it can be seen in Figure 11. It shows a skill score based on a relation between the mean squared error of the CCLM-VEG3D run and the mean squared error of the CCLM-TERRA-ML simulation, according to the following equation:

$$skill\ score = 1 - \frac{\Sigma(VEG3D - OBS)^2}{\Sigma(TERRA - OBS)^2} \quad (4.1)$$

VEG3D stands for the monthly precipitation sums in September over the decade 2001–2010 in the CCLM-VEG3D simulation, TERRA for the ones in the CCLM-TERRA-ML run. OBS denotes the observed rainfall amounts from the UDEL dataset for the same months. According to this equation, a positive skill score is achieved if the mean squared error of CCLM-VEG3D is lower than the one of CCLM-TERRA-ML. A higher deviation to the observations creates a negative skill score. Consequently, the reddish colours, representing positive skill score, indicate the areas where CCLM-VEG3D has an added value concerning the representation of the rainfall amounts, averaged over all September months in the decade 2001–2010. The blue colours indicate the re-

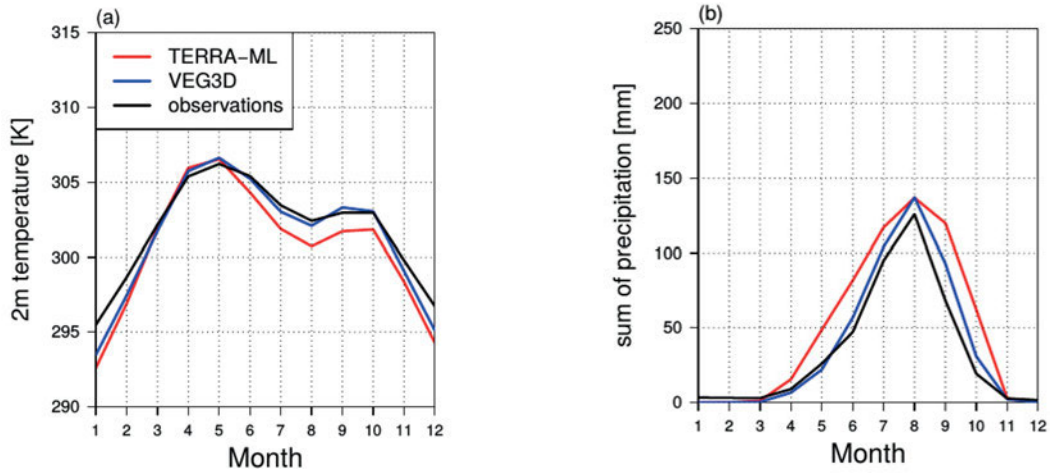


**Figure 8:** Annual cycle of area averaged monthly mean 2 m temperatures (a) and monthly mean precipitation sum (b) in Central Sahel for the years 2001–2010. The red line shows the result of the CCLM-TERRA-ML simulation, the blue one the result of the CCLM-VEG3D simulation. UDEL is given in black.

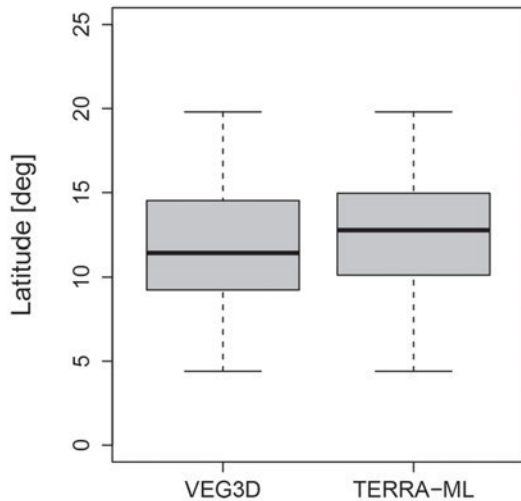


**Figure 9:** Latitudinal locations of the daily rainfall maxima in West Africa in September over the period 2001–2010 for the CCLM-TERRA-ML and the CCLM-VEG3D simulations. The thick black line represents the mean position of the daily rainfall maxima, the grey box comprises the 25- and the 75-Percentile, and the thin black lines define the whole spread of occurring latitudinal positions.

gions where CCLM-VEG3D has no added value. It can clearly be seen that the positive skill score dominate over West Africa and in the Sahel region. In about 68 % of all grid cells in this area CCLM-VEG3D has an added value. In 32 % it is as good as CCLM-TERRA-ML or has no added value. Thus, it can be stated that the interactions between soil, vegetation and atmosphere affect the spatial distribution of rainfall in the Sahel region also on the decadal timescale, and a more complex representation of these interactions within RCM simulations predominantly improves the simulated spatial rainfall distribution in West Africa. This effect is also reflected in

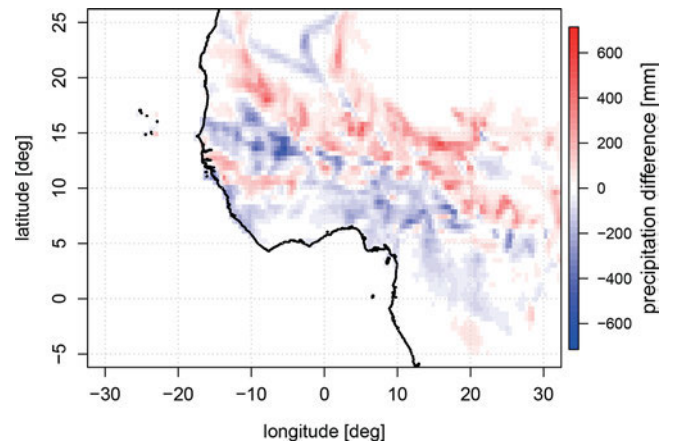


**Figure 10:** Mean differences in precipitation between the CCLM-TERRA-ML and the CCLM-VEG3D simulations in [mm] averaged over all Septembers in 2001–2010.

the improved spatially averaged annual cycle of the precipitation sums for the Central Sahel (Figure 8 (b)).

## 5 Discussion and conclusions

In this study two different SVATs, namely TERRA-ML and VEG3D, have been coupled to the regional climate model CCLM, and simulations have been performed to investigate the influence of the soil-vegetation-atmosphere interactions on the West African Monsoon system. In a sensitivity study for the year 1979 the differences in simulation results, due to the application of the two different SVATs, were analyzed, to identify relevant processes between the surface and the atmosphere, affecting the monsoon characteristics. Subsequently, these findings were validated on a decadal timescale by performing ERA-Interim driven simulation runs from 2001–2010. Analyses revealed that the soil-vegetation-atmosphere interactions considerably affect



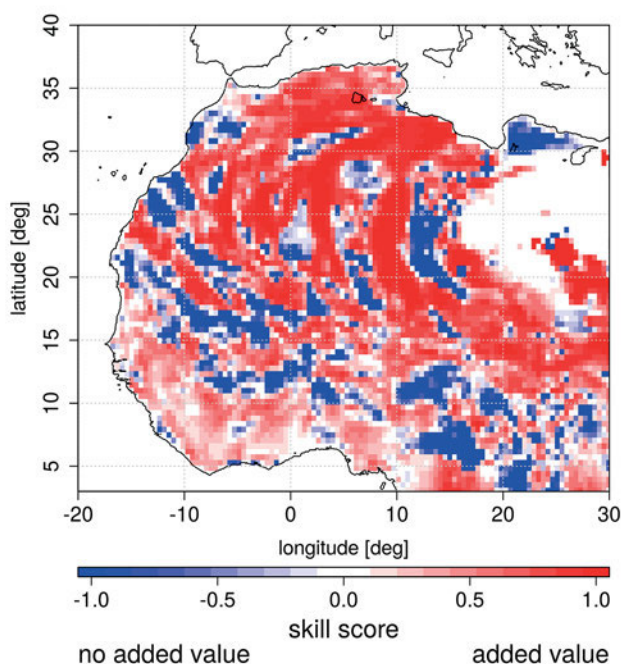


**Figure 11:** Added value of CCLM-VEG3D compared to CCLM-TERRA-ML concerning the representation of the rainfall amounts in September between 2001–2010.

the spatial distribution of rainfall in the Sahel region. The spatial differences in precipitation are triggered by differences in the structural design of the SVATs leading to warmer near surface temperatures in CCLM-VEG3D for the Central Sahel. Using the more complex SVAT VEG3D instead of TERRA-ML reduces the mean squared error of the monthly precipitation sums in West Africa substantially.

Comparing the results of CCLM-VEG3D and CCLM-TERRA-ML runs it could be shown that during the Sahelian rainy season between June and October higher near surface temperatures are simulated in the CCLM-VEG3D run. As a consequence the Saharian heat-low reaches farther south in the Sahel region, shifting the baroclinic zone in which the AEJ is formed to the south as well. This results in a southward displacement of the average AEJ position in the CCLM-VEG3D simulation. Thus, MCSs developing in connection with the AEJ during the monsoon season, move on southerly tracks through the Sahel region, producing less precipitation in the Central Sahel. This reduction in rainfall amount in the CCLM-VEG3D run matches much better to observations.

The CCLM experiments, which have been performed, differ only in the used SVATs. Therefore, deviations in simulation results must be caused by differences in the SVATs. One possible explanation for different simulation results is the consideration of a vegetation layer in VEG3D, which is missing completely in the structural design of TERRA-ML. This vegetation layer changes the treatment of radiation fluxes in CCLM-VEG3D. Wherever vegetation exists, the incom-

ing short-wave radiation at the surface is decreased due to shading by the vegetation, resulting in a lower heating of the soil. At the same time, the vegetation layer prevents a too strong cooling of the soil, by emitting long-wave radiation back to the ground depending on the temperature at the vegetation canopy. These physical mechanisms induced by the vegetation layer also affect the annual cycle of temperature and might be the reason for the reduced temperature amplitude in the CCLM-VEG3D simulation compared to the CCLM-TERRA-ML run.

Other possible reasons for the deviating temperatures are differences in the soil albedo that may change the characteristics of the Saharian heat low as described by KOTHE et al. (2014), and the different parameterizations of the soil heat conductivity between both SVATs. In VEG3D the heat conductivity depends on the amount of soil water, in the used TERRA-ML version this dependency is not taken into account. The potential of such a soil moisture dependent heat conductivity to affect the diurnal temperature cycle in West Africa is shown by SCHULZ et al. (2016), by including the approach of JOHANSEN (1977) into a more recent version of TERRA-ML. Since we were aware of this differences, an additional CCLM-TERRA-ML run with an implemented approach of JOHANSEN (1977) was performed, investigating its impact on the simulation results. The experiment revealed that the impact on the simulation results is small and lower as could be expected from SCHULZ et al. (2016). During summer, the temperature bias in CCLM-TERRA-ML was even increased when using the new TERRA-ML version. Thus, we consider the implemented vegetation layer in VEG3D as main factor for the temperature differences between CCLM-VEG3D and CCLM-TERRA-ML.

As a result of the structural differences between both SVATs, the near surface temperature in the Central Sahel, resulting from the CCLM-VEG3D simulation, is up to 1 K higher during the rainy season. These temperature differences between both experiments then affect, due to the chain of atmospheric processes described in Section 3, the spatial distribution of rainfall in the Sahel region.

The results of this study show that the soil-vegetation-atmosphere interactions may considerably influence the dynamics of the WAM. Thus, this study confirms the results of prior studies, and highlight the importance of the soil-vegetation-atmosphere interactions for the WAM development. For example in STEINER et al. (2009) a very similar process is described, whereby the use of a more sophisticated SVAT in RCM simulations reduced the meridional temperature gradient over Africa, shifting the AEJ to the south and improving the simulated precipitation for the Sahel region. Comparable results were found by XUE and SHUKLA (1996) and PATRICOLA and COOK (2008). Thus, the results of this study can smoothly be integrated into the existing concept of WAM dynamics. Additionally, they extend the knowledge about regional simulation of rainfall in the Sahel,

by highlighting the important role of a more complex description of vegetation in the structural design of SVATs. In consequence, it can be concluded that reliable predictions about the spatial variability of monsoon rainfall in the Sahel region can only be made if the interactions between soil, vegetation and atmosphere are captured reasonably within a RCM by a SVAT that describes the soil-vegetation-atmosphere interactions more realistically.

## Acknowledgments

We acknowledge funding from the Federal Ministry of Education and Research in Germany (BMBF) through the research programme MiKlip (FKZ: 01LP1518A). We acknowledge support by Deutsche Forschungsgemeinschaft and Open Access Publishing Fund of Karlsruhe Institute of Technology.

## References

- ADLER, B., N. KALTHOFF, L. GANTNER, 2011: The impact of soil moisture inhomogeneities on the modification of a mesoscale convective system: An idealised model study. – *Atmos. Res.* **101**, 354–372.
- ARAKAWA, A., V. LAMB, 1977: Computational design of the basic dynamical processes in the UCLA general circulation model. In: CHANG J. (ed.) *Methods in computational physics: general circulation models of the atmosphere*. Academic Press, New York, Vol. **17**, 173–265.
- BALDAUF, M., A. SEIFERT, J. FÖRSTNER, D. MAJEWSKI, M. RASCHENDORFER, T. REINHARDT, 2011: Operational convective-scale numerical weather prediction with the COSMO model: description and sensitivities. – *Mon. Wea. Rev.* **139**, 3887–3905. DOI:10.1175/MWR-D-10-05013.1.
- BARTHOLOME, E., A. BELWARD, 2005: GLC2000: a new approach to global land cover mapping from Earth observation data. – *Int. J. Remote Sens.* **26**, 1959–1977.
- BENSON, C., E.J. CLAY, 1998: The impact of drought on sub-Saharan African economies: a preliminary examination, Vol. 401. – *World Bank Publications*, Washington, 80 pp.
- BRAUN, F., 2005: Mesoskalige Modellierung der Bodenhydrologie. Dissertation, Universität Karlsruhe (TH), Institut für Meteorologie und Klimaforschung.
- BRAUN, F., G. SCHÄDLER, 2005: Comparison of soil hydraulic parameterizations for mesoscale meteorological models. – *J. Climate Appl. Meteor.* **44**, 1116–1132.
- DEARDORFF, J., 1978: Efficient prediction of ground surface temperature and moisture, with inclusion of a layer of vegetation. – *J. Geophys. Res.* **83**, 1889–1903.
- DEE, D., S.M. UPPALA, A.J. SIMMONS, P. BERRISFORD, P. POLI, S. KOBAYASHI, U. ANDRAE, M.A. BALMASEDA, G. BALSAMO, P. BAUER, and others, 2011: The ERA-Interim reanalysis: Configuration and performance of the data assimilation system. – *Quart. J. Roy. Meteor. Soc.*, **137** (656), 553–597.
- DICKINSON, R.E., 1984: Modeling evapotranspiration for three-dimensional global climate models. In: HANSEN J.E. and T. TAKAHASI (eds.): *Climate processes and climate sensitivity*. – *AGU Geophys. Monogr. Series*, **29**, 58–72, DOI:10.1029/GM029.
- DOMS, G., J. FÖRSTNER, E. HEISE, H.J. HERZOG, D. MIRONOV, M. RASCHENDORFER, T. REINHARDT, B. RITTER, R. SCHRODIN, J.P. SCHULZ, and others, 2011: A description of the nonhydrostatic regional COSMO model, Part I: Dynamics and Numerics. *Deutscher Wetterdienst*, Offenbach, Germany.
- GANTNER, L., N. KALTHOFF, 2010: Sensitivity of a modelled life cycle of a mesoscale convective system to soil conditions over West Africa. – *Quart. J. Roy. Meteor. Soc.* **136**, 471–482.
- GRABE, F., 2002: Simulation der Wechselwirkung zwischen Atmosphäre, Vegetation und Erdoberfläche bei Verwendung unterschiedlicher Parametrisierungsansätze. Dissertation, Universität Karlsruhe (TH), Institut für Meteorologie und Klimaforschung.
- HOLTON, J.R., G.J. HAKIM, 2013: *An introduction to dynamic meteorology*. – Academic press, Oxford, 532 pp.
- JOHANSEN, O., 1977: Thermal conductivity of soils. DTIC Document, Trondheim, 291 S.
- KAPTUE TCHUENTE, A.T., J.-L. ROUJEAN, S. FAROUX, 2010: ECOCLIMAP-II: An ecosystem classification and land surface parameters database of Western Africa at 1 km resolution for the African Monsoon Multidisciplinary Analysis (AMMA) project. – *Remote Sens. Env.* **114**, 961–976.
- KOHLER, M., G. SCHÄDLER, L. GANTNER, N. KALTHOFF, F. KÖNIGER, C. KOTTMEIER, 2012: Validation of two SVAT models for different periods during the West African monsoon. – *Meteorol. Z.* **21**, 509–524.
- KOSTER, R.D., P.A. DIRMEYER, Z. GUO, G. BONAN, E. CHAN, P. COX, C.T. GORDON, S. KANAE, E. KOWALCZYK, E. LAWRENCE, and others, 2004: Regions of strong coupling between soil moisture and precipitation. – *Science*, **305** (5687), 1138–1140.
- KOTHE, S., H.-J. PANITZ, B. AHRENS, 2014: Analysis of the radiation budget in regional climate simulations with COSMO-CLM for Africa. – *Meteorol. Z.* **23**, 123–141. DOI:10.1127/0941-2948/2014/0527.
- LARE, A., S. NICHOLSON, 1994: Contrasting conditions of surface water balance in wet years and dry years as a possible land surface-atmosphere feedback mechanism in the West African Sahel. – *Climate* **7**, 653–668.
- LARSON, J., R. JACOB, E. ONG, 2005: The Model Coupling Toolkit: A new Fortran90 toolkit for building multiphysics parallel coupled models. – *Int. J. High Performance Comp. Appl.* **19**, 277–292.
- LEBEL, T., A. DIEDHIOU, H. LAURENT, 2003: Seasonal cycle and interannual variability of the Sahelian rainfall at hydrological scales. – *J. Geophys. Res.* **108**, 8389, DOI:10.1029/2001JD001580.
- LENZ, C.J., 1996: Energieumsätze an der Erdoberfläche in gegliedertem Gelände. Dissertation, Universität Karlsruhe (TH), Institut für Meteorologie und Klimaforschung.
- MEISSNER, C., 2008: High-resolution sensitivity with the regional climate model COSMO-CLM. Dissertation, Universität Karlsruhe (TH), Institut für Meteorologie und Klimaforschung.
- MELLOR, G.L., T. YAMADA, 1982: Development of a turbulence closure model for geophysical fluid problems. – *Rev. Geophys.* **20**, 851–875.
- MITCHELL, T.D., P.D. JONES, 2005: An improved method of constructing a database of monthly climate observations and associated high-resolution grids. – *Int. J. Climatol.* **25**, 693–712. DOI:10.1002/joc.1181.
- MORTIMORE, M., 1989: *Adapting to drought: Farmers, famines, and desertification in West Africa*. – Cambridge University Press, Cambridge, 299 pp.
- NICHOLSON, S., 2013: *The West African Sahel: A review of recent studies on the rainfall regime and its interannual variability*. – *ISRN Meteorology*, 2013, 453521 (32 pp.).
- NICHOLSON, S., J.P. GRIST, 2003: The seasonal evolution of the atmospheric circulation over West Africa and equatorial Africa. – *J. Climate* **16**, 1013–1030.
- NICHOLSON, S., I.M. PALAO, 1993: A re-evaluation of rainfall variability in the sahel. Part I. Characteristics of rainfall fluctuations. – *Int. J. Climatol.* **13**, 371–389.

- PAL, J.S., E.A. ELTAHIR, 2001: Pathways relating soil moisture conditions to future summer rainfall within a model of the land-atmosphere system. – *J. Climate* **14**, 1227–1242.
- PANITZ, H.-J., A. DOSIO, M. BÜCHNER, D. LÜTHI, K. KEULER, 2014: COSMO-CLM (CCLM) climate simulations over CORDEX-Africa domain: analysis of the ERA-Interim driven simulations at 0.44 and 0.22 resolution. – *Climate Dyn.* **42**, 3015–3038.
- PARKER, D., E. GOOD, R. CHADWICK, 2012: Reviews of observational data available over Africa for monitoring, attribution and forecast evaluation. – Hadley Centre Technical Note **86**.
- PATRICOLA, C., K.H. COOK, 2008: Atmosphere/vegetation feedbacks: A mechanism for abrupt climate change over northern Africa. – *J. Geophys. Res.* **113**, D18102, DOI: [10.1029/2007JD009608](https://doi.org/10.1029/2007JD009608).
- PHILIPPON, N., B. FONTAINE, 2002: The relationship between the Sahelian and previous 2nd Guinean rainy seasons: a monsoon regulation by soil wetness? – *Annales Geophysicae* **20**, 575–582.
- RASCHENDORFER, M., 2001: The new turbulence parameterization of LM. – *COSMO newsletter* **1**, 89–97.
- REED, R.J., D.C. NORQUIST, E.E. RECKER, 1977: The structure and properties of African wave disturbances as observed during Phase III of GATE. – *Mon. Wea. Rev.* **105**, 317–333.
- RIJTEMA, P., 1969: Soil moisture forecasting. – Instituut voor Cultuurtechniek en Waterhuishouding, Wageningen, 513 pp.
- RITTER, B., J.-F. GEYLEN, 1992: A comprehensive radiation scheme for numerical weather prediction models with potential applications in climate simulations. – *Mon. Wea. Rev.* **120**, 303–25.
- ROCKEL, B., A. WILL, A. HENSE, 2008: The regional climate model COSMO-CLM (CCLM). – *Meteorol. Z.* **17**, 347–348. DOI: [10.1127/0941-2948/2008/0309](https://doi.org/10.1127/0941-2948/2008/0309).
- RUDOLF, B., A. BECKER, U. SCHNEIDER, A. MEYER-CHRISTOFFER, M. ZIESE, 2010: The new GPCC full data reanalysis Version 5 providing high-quality gridded monthly precipitation data for the global land-surface is public available since December 2010. – GPCC status report December 1–7.
- SCHÄDLER, G., 1990: Numerische Simulationen zur Wechselwirkung zwischen Landoberfläche und atmosphärischer Grenzschicht. Dissertation, Universität Karlsruhe (TH), Institut für Meteorologie und Klimaforschung.
- SCHÄR, C., D. LÜTHI, U. BEYERLE, E. HEISE, 1999: The soil-precipitation feedback: A process study with a regional climate model. – *J. Climate* **12**, 722–741.
- SCHRODIN, E., E. HEISE, 2002: A new multi-layer soil model. – *COSMO newsletter* **2**, 149–151.
- SCHULZ J.-P., G. VOGEL, C. BECKER, S. KOTHE, U. RUMMEL, A. AHRENS, 2016: Evaluation of the ground heat flux simulated by a multi-layer land surface scheme using high-quality observations at grass land and bare soil. – *Meteorol. Z.*, **25**, 607–620, DOI: [10.1127/metz/2016/0537](https://doi.org/10.1127/metz/2016/0537)
- SEIFERT A., K.D. BEHENG, 2001: A double-moment parameterization for simulating autoconversion, accretion and selfcollection. – *Atmos. Res.* **59-60**, 265–281.
- STEINER, A.L., J.S. PAL, S.A. RAUSCHER, J.L. BELL, N.S. DIFENBAUGH, A. BOONE, L.C. SLOAN, F. GIORGI, 2009: Land surface coupling in regional climate simulations of the West African monsoon. – *Clim. Dyn.* **33**, 869–892.
- STULL, R.B., 2012: An introduction to boundary layer meteorology (Vol. 13). – Springer Science & Business Media.
- TAYLOR, C.M., D.J. PARKER, C.R. LLOYD, C.D. THORNCROFT, 2005: Observations of synoptic-scale land surface variability and its coupling with the atmosphere. – *Quart. J. Roy. Meteor. Soc.* **131**, 913–937.
- TEULING, A., S. SENEVIRATNE, C. WILLIAMS, P. TROCH, 2006: Observed timescales of evapotranspiration response to soil moisture. – *Geophys. Res. Lett.* **33**, L23403, DOI: [10.1029/2006GL028178](https://doi.org/10.1029/2006GL028178).
- TIEDTKE, M., 1989: A comprehensive mass flux scheme for cumulus parameterization in large-scale models. – *Mon. Wea. Rev.* **117**, 1779–1800.
- UPPALA, S.M., P.W. KALLBERG, A.J. SIMMONS, U. ANDRAE, V. BECHTOLD, M. FIORINO, J.K. GIBSON, J. HASELER, A. HERNANDEZ, G.A. KELLY, and others, 2005: The ERA-40 reanalysis. – *Quart. J. Roy. Meteor. Soc.*, **131** (612), 2961–3012.
- VALCKE, S., 2013: The OASIS3 coupler: a European climate modelling community software. – *Geosci. Model Dev.* **6**, 373–388.
- VALCKE, S., T. CRAIG, L. COQUART, 2013: OASIS3-MCT User Guide OASIS3-MCT 2.0. – Technical Report, TR/CMGC/13/17, CERFACS/CNRS SUC URA.
- VAN GENUCHTEN M.T., 1980: A closed-form equation for predicting the hydraulic conductivity of unsaturated soils. – *Soil Sci. Soc. Amer. J.* **44**, 892–898.
- WILL, A., N. AKHTAR, J. BRAUCH, M. BREIL, E. DAVIN, H. HOHAGEMANN, E. MAISONNAVE, M. THÜRKOW, S. WEIHER, 2017: The COSMO-CLM 4.8 regional climate model coupled to regional ocean, land surface and global earth system models using OASIS3-MCT: description and performance. – *Geosci. Model Dev.* **10**, 1549–1586, DOI: [10.5194/gmd-10-1549-2017](https://doi.org/10.5194/gmd-10-1549-2017).
- WICKER L.J., W.C. SKAMAROCK, 2002: Time-splitting methods for elastic models using forward time schemes. – *Mon. Wea. Rev.* **130**, 2088–2097.
- WILLMOTT, C., K. MATSUURA, 1998: Global air temperature and precipitation: Regrided monthly and annual climatologies (version 2.01). – Univ. of Delaware, Newark, U.S.A.
- XUE Y., J. SHUKLA, 1996: The influence of land surface properties on Sahel climate. Part II. Afforestation. – *J. Climate* **9**, 3260–3275.
- ZHANG, Q., H. KÖRNICH, K. HOLMGREN, 2012: How well do re-analyses represent the southern African precipitation? – *Clim. Dyn.* **40**, 951–962, DOI: [10.1007/s00382-012-1423-z](https://doi.org/10.1007/s00382-012-1423-z).